

Designing evanescent optical interactions to control the expression of Casimir forces in optomechanical structures

Alejandro W. Rodriguez,^{1,2} David Woolf,¹ Pui-Chuen Hui,¹ Eiji Iwase,¹ Alexander P. McCauley,³ Federico Capasso,¹ Marko Loncar,¹ and Steven G. Johnson²

¹*School of Engineering and Applied Sciences, Harvard University, Cambridge, MA 02139*

²*Department of Mathematics, Massachusetts Institute of Technology, Cambridge, MA 02139*

³*Department of Physics, Massachusetts Institute of Technology, Cambridge, MA 02139*

We propose an optomechanical structure consisting of a photonic-crystal (holey) membrane suspended above a layered silicon-on-insulator substrate in which resonant bonding/antibonding optical forces created by externally incident light from above enable all-optical control and actuation of stiction effects induced by the Casimir force. In this way, one can control how the Casimir force is expressed in the mechanical dynamics of the membrane, not by changing the Casimir force directly but by optically modifying the geometry and counteracting the mechanical spring constant to bring the system in or out of regimes where Casimir physics dominate. The same optical response (reflection spectrum) of the membrane to the incident light can be exploited to accurately measure the effects of the Casimir force on the equilibrium separation of the membrane.

Casimir forces between neutral objects arise due to quantum and thermal fluctuations of the electromagnetic field and, being ordinarily attractive, can contribute to the failure (stiction) of micro-electromechanical systems (MEMS)^{1–3}. In this letter, we propose a scheme for controlling and measuring the Casimir force between a photonic-crystal membrane and a layered substrate that exploits the resonant optomechanical forces created by evanescent fields^{4–6} in response to external, normally incident light⁷. Our numerical experiments reveal a sensitive relationship between the equilibrium separation of the membrane and the Casimir force, as well as demonstrate low-power optical control over stiction effects. (Although our focus is on stiction induced by the Casimir force, similar results should also apply in circumstances involving electrostatic forces)¹. Casimir forces have most commonly been measured in cantilever experiments involving sphere–plate geometries^{1,8,9}, with some exceptions¹⁰, in which the force is often determined by measuring its gradient as a function of object separation. Another approach involves measuring the dynamic response of a plate to mechanical modulations induced by an electrostatic voltage^{1,11}. Here, we consider an alternative scheme in which the Casimir force is determined instead via *pump–probe* measurements of the optically tunable equilibrium separation between a membrane and a substrate, a proof of concept of an approach to all-optical control and actuation of opto-micromechanical devices susceptible to stiction^{1,3,12,13}.

We focus on the optomechanical structure shown in Fig. 1, and which we first examined in Ref. 7: a silicon membrane of thickness $h = 130$ nm and width $W = 23.4$ μm perforated with a square lattice of air holes of diameter 260 nm and period 650 nm, suspended above a layered substrate—a silicon film of thickness $h = 130$ nm on a silica (SOI) substrate—by four rectangular supports of length $L = 35$ μm and cross-sectional area 130 nm \times 2 μm .

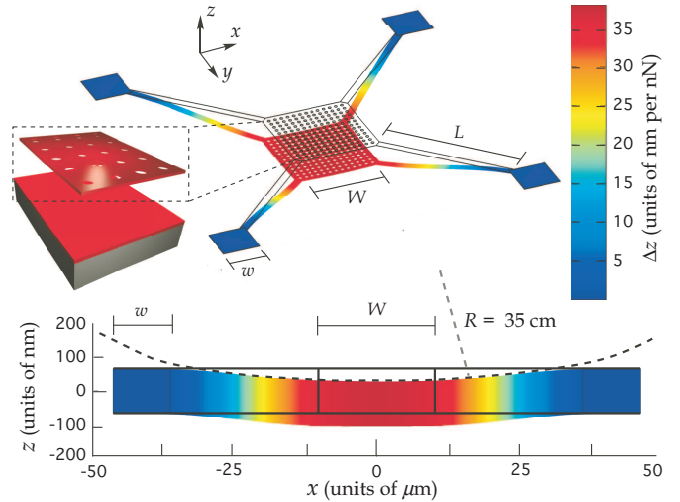


FIG. 1. Schematic of single-membrane structure (thickness $h = 130$ nm and size $W = 23.4$ μm), designed so that normally incident light from above ($+z$ direction) induces resonant optical forces on the membrane. Also shown is a color-bar of the membrane displacement due to an impinging 1 nN force. Notice that the arms supporting the membrane (length $L = 35$ μm) bend significantly more than the membrane: the total bending of the membrane is ≈ 38 nm, while the membrane’s center–corner height difference is a mere 2.7 nm, corresponding to an effective radius of curvature $R \approx 35$ cm.

In what follows, we consider quasistatic membrane deformations induced by static (and spatially uniform) optical/Casimir forces, so it suffices to study the fundamental mechanical mode and corresponding frequency Ω_m of the membrane. The mode profile is illustrated in Fig. 1 and consists of an approximately flat membrane with deformed supports, making this structure less susceptible to optical losses stemming from curvature [Fig. 1 caption]. For the particular configuration studied here, we found

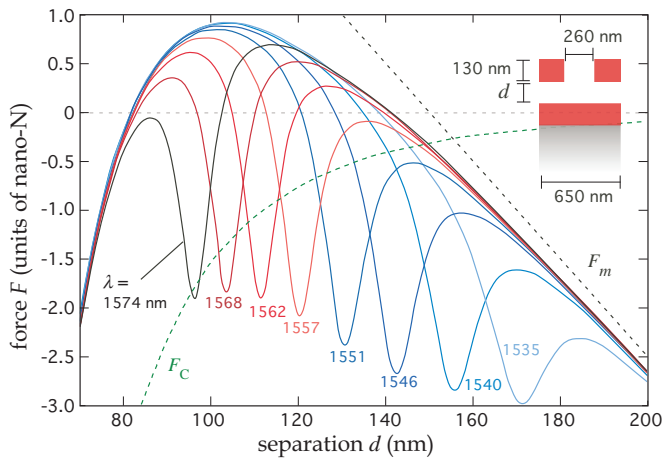


FIG. 2. Total force $F = F_m + F_c + F_o$ on the membrane of Fig. 1 (cross-section shown on the inset), initially suspended at $d_0 = 150$ nm, as a function of membrane separation d . F_m is the mechanical restoring force (dashed black), F_c the Casimir force (dashed green) and F_o the optical force induced by normally-incident light of power $P = 10$ mW and wavelength λ . F is plotted for different λ .

$\Omega_m \approx 63$ kHz, corresponding to a mechanical spring constant $\kappa_m \approx 5 \times 10^{-2}$ N/m.

Away from a desired initial mechanical membrane-surface separation d_0 , here chosen to be $d_0 = 150$ nm, and in the absence of optical forces, the membrane will experience two forces, plotted in Fig. 2 as a function of separation d : a restoring mechanical force $F_m = \kappa_m(d_0 - d)$ that increases linearly with separation d (dashed black line), and the attractive, monotonically-decaying Casimir force F_c (dashed green line). F_c was computed via the standard proximity-force approximation^{8,14}, which we have checked against exact time-domain calculations^{15,16} and found to be accurate to within 3%. F_c has two major effects on the membrane: First, it leads to a new equilibrium separation $d_c \approx 140$ nm; Second, it creates an unstable equilibrium at a smaller separation $d_u \approx 80$ nm, determined by the competition between F_m and F_c , below which the membrane will stick to the substrate. We propose that the Casimir force can be measured by optically controlling the equilibrium separation in real time by illuminating the membrane with normally incident light at a tunable wavelength λ , which creates a resonant force and allows one to dynamically determine the Casimir-induced threshold for stiction⁷. In particular, Fig. 2 also plots the total force on the membrane $F = F_m + F_c + F_o$, where F_o is the single- λ optical force on the membrane induced by incident light of power $P = 10$ mW. Here, the strong λ -dependence of F_o is exploited to obtain large and tunable attractive (bonding) forces at any desired d (solid lines), allowing us to control the equilibrium separation of the membrane⁷. As shown, slowly increasing λ from $\lambda \approx 1520$ nm to $\lambda \approx 1581$ nm causes d_c to decrease and come arbitrarily close to d_u .

Figure 3 quantifies the effect of F_o and F_c on the equi-

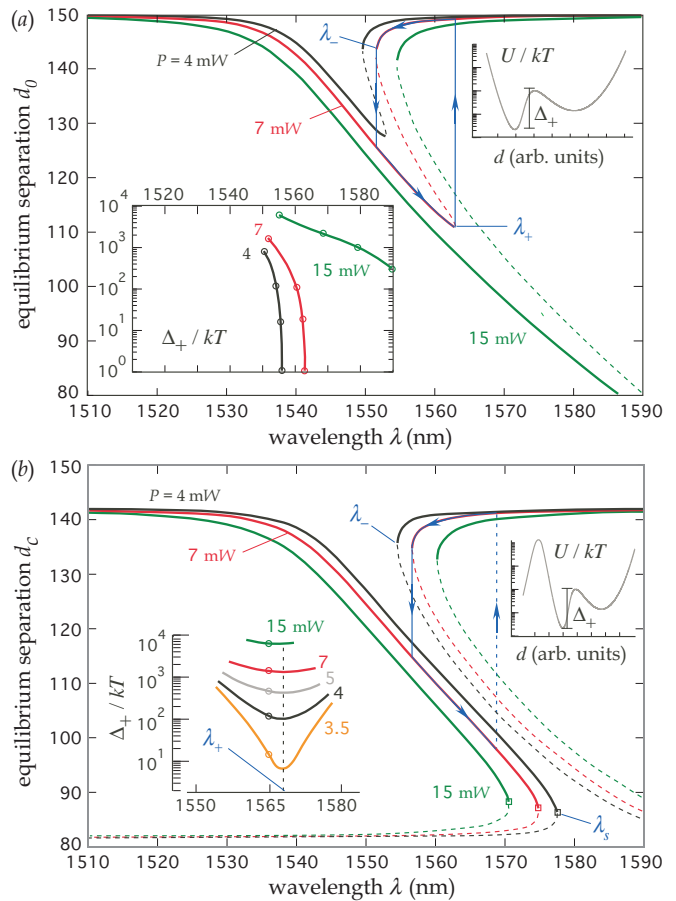


FIG. 3. Stable (solid) and unstable (dashed) membrane equilibrium separations in response to normally-incident light of power P , as a function of optical wavelength λ , plotted for multiple P , excluding (a) and including (b) the Casimir force F_c . The right insets are schematic illustrations of the energy landscape as a function of membrane separation d , indicating the energy barrier Δ_+/kT separating the lower and higher stable equilibria. The left insets plot Δ_+/kT as a function of λ plotted for multiple P .

librium of the membrane. In particular, Fig. 3(a) and Fig. 3(b) plot the equilibrium separation, d_c and d_o , in the absence ($F_c = 0$) and presence ($F_c \neq 0$) of the Casimir force, respectively, as a function of $\lambda \in [1510, 1590]$ nm, for light incident at various P . When $F_c = 0$ [Fig. 3(a)], increasing λ has two main effects on the membrane: First, the equilibrium separation decreases; Second, two bifurcation wavelengths, denoted by λ_{\pm} (indicated in the figure), are created due to the presence of two additional (stable and unstable) equilibria, leading to bistability and hysteresis effects as λ is varied^{3,17}. This is illustrated by the blue curve in the particular case of $P = 7$ mW: if λ is slowly increased from $\lambda \approx 1510$ nm, d_o decreases until $\lambda \rightarrow \lambda_+ \approx 1562$ nm, at which point the stable and unstable equilibria bifurcate and the position of the membrane changes dramatically from $d_o = 112$ nm to $d_o \approx 150$ nm. Decreasing λ below λ_+ after the transition causes the membrane to transverse a different path, leading to an-

other dramatic change in d_o as $\lambda \rightarrow \lambda_- \approx 1551$ nm from above. The same is true at other P , although of course the corresponding λ_{\pm} will change. The presence of $F_c > 0$ [Fig. 3(b)] affects the membrane's response to F_o in important ways: For small P , F_o is too weak and therefore d_c is too large for F_c to have a strong effect on the membrane (the membrane reaches λ_+ before it can feel the Casimir force). At larger $P > P_c \approx 3$ mW, however, d_c and λ_- are greatly affected by F_c and there is no longer any optical bistability: the bifurcation point λ_+ is instead replaced with a new bifurcation point $\lambda_s > \lambda_+$, arising from the lower (stable) and Casimir-induced (unstable) equilibria, leading to stiction rather than a jump in the membrane separation as $\lambda \rightarrow \lambda_s$.

In an experiment, the presence of Brownian motion will cause membrane fluctuations about the stable equilibria, and these can lead to dramatic transitions in the position of the membrane, from one stable equilibrium to another, and even to stiction, as the membrane moves past the energy barrier Δ separating the various stable equilibria; the right insets of Fig. 3 illustrate the energy landscape of the membrane. The average lifetime τ of a metastable equilibrium is proportional to $\exp(\Delta/kT)$, which explains why they are rarely observed in stiff mechanical systems where $\Delta/kT \gg 1$,³ but in our case τ can be made arbitrarily small by exploiting F_o : the barrier Δ_{\pm} between the two stable equilibria $\rightarrow 0$ as $\lambda \rightarrow \lambda_{\pm}$, as shown by the left inset of Fig. 3(a). The presence of F_c has a dramatic effect on these thermally induced transitions. In particular, even though there is no bifurcation point λ_+ , the barrier from the smallest to larger stable d_c (denoted by Δ_+) can be made arbitrarily small and varies non-monotonically with λ : as λ is increased from $\lambda_- \rightarrow \lambda_s$, Δ_+ decreases and then increases as λ passes through a critical λ_+ [indicated in Fig. 3(b)]. This potential “dip” gets deeper as P decreases [as shown in the left inset of Fig. 3(b)], making it easier for the membrane to transition to the larger d_c . Thus, for sufficiently small P , the *rate* at which λ is increased determines whether the membrane transitions upwards near λ_+ or sticks to the substrate near λ_s : if $d\lambda/dt \gg \lambda/\tau$ near λ_+ , the upward transition is “frustrated”. This creates a hysteresis effect [illustrated by the blue curve in Fig. 3(b)] where the upward transition (dashed blue line) can occur only due to thermal fluctuations and whether or not this occurs will depend on P and $d\lambda/dt$. For P smaller than a critical $P_c \approx 3$ mW, the lower stable and higher unstable d_c merge, leading to two additional bifurcations (not shown), and it becomes impossible to continuously change λ to obtain a transition from stable suspension into stiction [instead, the optical bistability behavior of Fig. 3(a) is observed]. This ability to tune the stiction barrier through F_o remains an unexplored avenue for experimentally gauging the impact of Casimir and other stiction forces on the operation of optomechanical systems.

Our results thus far demonstrate a sensitive dependence of d_c on F_c and λ . However, determining F_c accu-

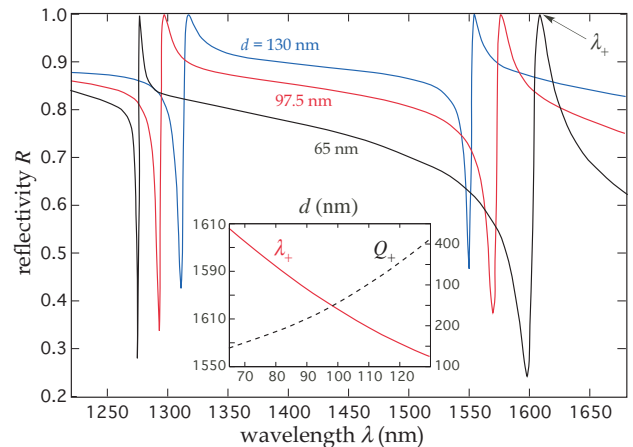


FIG. 4. Reflectivity R as a function of optical wavelength λ at various membrane separations d . The inset shows the peak wavelength λ_+ (solid red) and lifetime Q_+ (dashed black) as a function of d .

rately rests on the ability to determine d_c accurately, and we propose to measure the latter interferometrically via the (broadband) optical response of the membrane⁷. Figure 4 plots the reflectivity R of the membrane as a function of λ at various d , showing the presence of multiple reflection peaks at positions λ_{\pm} (indicated in the figure) that shift as d is varied—these correspond to the bonding (+) and antibonding (−) resonances that allowed us earlier to control the membrane’s equilibrium separation. The inset plots the λ_+ and corresponding lifetime Q_+ of the bonding mode as d is varied, revealing a large change in $d\lambda_+/dd \in [0.5, 1.2]$ and $dQ_+/dd \in [5, 12]$ nm^{−1} over the entire d -range.

The basic phenomena described here are by no means limited to the particular realization of this geometry, nor to our choice of initial equilibrium position, and we believe that similar and more pronounced effects should be present in other configurations. For example, dramatically lower P can be obtained by increasing the Q of the membrane resonances, beyond the mere $Q \sim 10^2$ here, e.g. by decreasing the radii of the air holes (limited by losses). We note that antibonding (repulsive) forces can also be exploited, in conjunction with bonding forces, to overcome prohibitive stiction effects in similar optomechanical systems¹⁸, e.g. as an antistiction feedback mechanism⁷.

This work was supported by the Defense Advanced Research Projects Agency (DARPA) under contract N66001-09-1-2070-DOD.

¹F. Capasso, J. N. Munday, D. Iannuzzi, and H. B. Chan, *IEEE J. Select. Top. Quant. Electron.* **13**, 400–415 (2007).

²F. M. Serry, D. Walliser, and M. G. Jordan, *J. Appl. Phys.* **84**, 2501–2506 (1998).

³E. Buks and M. L. Roukes, *Europhys. Lett.* **54**, 220 (2001).

⁴M. L. Povinelli, M. Loncar, M. Ibanescu, E. J. Smythe, S. G. Johnson, F. Capasso, and J. D. Joannopoulos, *Opt. Lett.* **30**, 3042 (2005).

- ⁵T. J. Kippenberg and K. J. Vahala, *Science* **321**, 1172–1176 (2008).
- ⁶D. V. Thourhout and J. Roels, *Nature Photonics* **4**, 211–217 (2010).
- ⁷A. W. Rodriguez, A. P. McCauley, P. Hui, D. Woolf, E. Iwase, F. Capasso, M. Loncar, and S. G. Johnson, *Opt. Express* **19**, 2225–2241 (2011).
- ⁸K. A. Milton, *J. Phys. A* **37**, R209–R277 (2004).
- ⁹S. K. Lamoreaux, *Rep. Prog. Phys.* **68**, 201–236 (2005).
- ¹⁰A. W. Rodriguez, F. Capasso, and S. G. Johnson, *Nat. Phot.* **5**, 211–221 (2011).
- ¹¹H. B. Chan, V. A. Aksyuk, R. N. Kleinman, D. J. Bishop, and F. Capasso, *Phys. Rev. Lett.* **87**, 211801 (2001).
- ¹²S. Manipatruni, J. T. Robinson, and M. Lipson, *Phys. Rev. Lett.* **102**, 213903 (2009).
- ¹³W. H. P. Pernice, M. Li, D. Garcia-Sanchez, and H. X. Tang, *Opt. Express* **18**, 12615–12621 (2010).
- ¹⁴C. Genet, A. Lambrecht, and S. Reynaud, *Eur. Phys. J. Special Topics* **160**, 183–193 (2008).
- ¹⁵A. W. Rodriguez, A. P. McCauley, J. D. Joannopoulos, and S. G. Johnson, *Phys. Rev. A* **80**, 012115 (2009).
- ¹⁶A. P. McCauley, A. W. Rodriguez, J. D. Joannopoulos, and S. G. Johnson, *Phys. Rev. A* **81**, 012119 (2010).
- ¹⁷A. Dorsel, J. McCullen, P. Meystre, E. Vignes, and H. Walther, *Phys. Rev. Lett.* **51**, 1550–1553 (1983).
- ¹⁸R. Maboudian and R. Howe, *Tribology Letters* **3**, 215–221 (1997).